JSLHR JOURNAL OF SPEECH, LANGUAGE, AND HEARING RESEARCH

Quantifying tongue tip shape in apical and laminal /s/: contributions of palate shape

Journal:	*Journal of Speech, Language, and Hearing Research*
Manuscript ID	JSLHR-S-19-0114.R1
Manuscript Type:	Research Article
Date Submitted by the Author:	n/a
Complete List of Authors:	Stone, Maureen; University of Maryland School of Dentistry, Biomedical Sciences Gomez, Arnold; Johns Hopkins University, Dept. Electrical and Computer Engineering Zhuo, Jiachen; University of Maryland Medical System, Diagnostic Radiology Tchouaga, Ange; University of Maryland School of Dentistry, Neural and Pain Sciences Prince, Jerry; Johns Hopkins University, Dept. Electrical and Computer Engineering
Keywords:	Speech, Speech production, Articulation, Adults

Note: The following files were submitted by the author for peer review, but cannot be converted to PDF. You must view these files (e.g. movies) online.

curvatureCalc.m
fitcircle.m
fitcircle3D.m
main.m

Quantifying tongue tip shape in apical and laminal /s/: contributions of palate shape

Maureen Stone

University of Maryland School of Dentistry, Dept of Neural and Pain Sciences,

Orthodontics and Pediatrics, 650 W. Baltimore St, Baltimore MD, 21201, USA.

Tel: 410-706-1269, email: mstone@umaryland.edu

Arnold D. Gomez

Johns Hopkins University, Dept of Electrical and Computer Engineering, Baltimore, MD

Jiachen Zhuo

University of Maryland School of Medicine, Dept of Radiology, Baltimore, MD

Ange Lydie Tchouaga

University of Maryland School of Dentistry, Dept of Neural and Pain Sciences,

Baltimore, MD

Jerry L. Prince

Johns Hopkins University, Dept of Electrical and Computer Engineering, Baltimore, MD

Submission date: March 12, 2019

Running Title: Quantifying apical and laminal /s/

Abstract

Purpose. Anterior tongue shape during /s/ production is often described as "tip-up" or apical, versus "tip-down" or laminal. Typically, this is determined by observing the shape of the anterior midline tongue. The purpose of this study was to identify methods of curvature calculation that quantify the observed shape differences and to examine whether the shape differences were affected by palate shape. Previous work shows that palate height has some effect (Grimm, et al., 2017).

Method. Four curvature-based measures were applied to a series of points selected along the tongue surface in midsagittal cine-MR images during speech. The measures were minimal curvature, averaged largest curvature (ALC), normalized ALC, and interpolated normalized ALC. These measures were compared to visual judgments of apical and laminal /s/. Anterior palate shape was measured from dental casts.

Results. The apical /s/ contained a flat or concave region in the anterior tongue, while the laminal /s/ had a convex shape along the entire tongue. Thus, the laminal shape was less complex than the apical. The last two metrics, based on averages of multiple normalized curvatures, captured this complexity difference. Subjects with a more steeply sloped anterior palate tended to use laminal /s/.

Conclusion. The tongue shape for the two /s/-types was best defined by complexity of the shape, rather than local anterior shape. Statistical quantities that measured curvature in multiple locations, and normalized across subjects, were best at distinguishing the two /s/ shapes. Interpolating additional points between the manually selected ones did not improve the method.

Keywords: tongue shape; apical laminal; MRI

INTRODUCTION

The primary goal of this study is to create a simple, clinically useful method, based on curvature, to objectively quantify midsagittal tongue shape during apical and laminal /s/. The midsagittal tongue was chosen as the measurement site, because the midline vocal tract shape is the best single representative of the 3D vocal tract contour, and because 2D midline data sets are available to researchers more often than 3D data sets. The anterior tongue was measured because it executes the linguo-alveolar constriction used in /s/. Several curvature methods were tested to determine the one that best captures the shape features used by human observers (raters) when categorizing /s/-type from MRI images. In addition, we considered whether midline palate shape, that is, anterior slope and convexity, affect anterior tongue shape and choice of /s/-type.

Apical and Laminal /s/

The tongue shape during /s/ is a funnel, wider at back, which focuses and narrows the airstream into the alveolar constriction and onto the anterior teeth (cf. Stone and

Lundberg, 1996), There are two types of /s/ production, apical and laminal (see Dart, 1991). For both types, the sides of the tongue contact the lateral palate and inner surface of the teeth, producing a tongue groove along the vocal tract midline to direct the air stream toward the incisors. The key difference between the two productions occurs in the anterior tongue. The apical /s/ creates the alveolar constriction with the tongue tip, while the laminal /s/ uses the tongue blade (Dart, 1991) (see Figure 1). Apical and laminal tongue motions are usually categorized subjectively by direct observation of the tongue shape in a midsagittal tongue image (cf. Dart 1998).

The use of apical or laminal /s/-type, has been thought historically to be idiosyncratic and somewhat random across speakers. There is no audible acoustic or perceptual difference between the two /s/-types (Stoner, Gately and Rivers, 1987, Dart, 1991, 1998). In addition, there is little evidence of languages preferring one type of /s/. Dart (1998) studied /s/-type in 20 English and 21 French speakers based on palatograms and linguagrams. She found 58% of American English speakers and 68% of French speakers used laminal /s/. Icht and Ben David (2017) used self-report to categorize /s/-

type in 100 Hebrew speakers. They found about 60% used laminal /s/ with no effect of age, gender, or country of birth. Understanding the differences between /s/-types is useful when training speakers to produce a correct /s/, however. It is easier for a patient to correct their /s/ in the direction of their natural preference, apical or laminal.

Quantification of Tongue Surface Shape

Tongue shape differences due to phoneme categories have been quantified from ultrasound images of the midsagittal tongue. Curvature signatures and polynomial functions quantify global tongue shapes in isolation, because ultrasound images do not capture other vocal tract features (Morrish et al., 1984, 1985). A combination of curvature signatures and polynomial functions comprise the Curvature Index (CI) (Stolar and Gick, 2013). The CI method applies a seventh order fit to a tongue surface contour, and then integrates the curvature of every point in the fit to create a single quantity representing tongue shape complexity. That study found that the /s/ and /z/ midsagittal tongue shapes are among the lowest in shape complexity for English phonemes; the study did not examine apical and laminal contrasts. In another study, Dawson, et al., (2016) compared a modified curvature index (MCI) to a Procrustes analysis (translation, rotation, scaling), and Fourier analysis (DFT) of ultrasound tongue shapes. The three methods were all successful at labeling tongue shape complexity, with DFT being the best. Principal components analysis (PCA) also provided good success in eliminating noise effects and facilitate quantification of tongue shapes from ultrasound images (cf. Harshman, Ladefoged and Goldstein, 1977, Slud et al., 2002, Hoole and Pouplier, 2017).

The present study is interested in subtle, local tongue shape differences between /s/-types, not the global effects of phonemic categories. The study uses MRI because it does a good job at imaging the anterior tongue, where the /s/-constriction and the apical/laminal differences are located. MRI has had more success in distinguishing apical and laminal /s/ than ultrasound. Narayanan et al., (1995) used MRI to study /s/-type, and found that apical fricatives showed deeper grooving behind the constriction than laminal ones. Our study aims to develop a quantity that captures subtle and local differences between laminal and apical /s/, which may include tongue shape complexity, and which should be applicable to distinguishing other sounds that differ in only one region of the tongue.

Palate Effects.

Our previous studies of /s/-type used MRI and dental casts to identify effects of palate height on /s/-type. Stone et al. (2013) and Grimm et al. (2017) compared palate vault height to /s/-type for single words in glossectomy patients and healthy controls. They showed that controls with low palates tended to use apical /s/, while those with high palates tended to use laminal /s/. It is possible that a low palate does not provide sufficient clearance for the tongue body elevation observed in laminal /s/. Alternatively, palate height could change the aerodynamics of the airflow into the constriction, thus affecting the nature of /s/ production.

Studies of palate doming offer another perspective on the effects of the hard palate on tongue behavior. Palate doming combines palate height and width, often by fitting a quadratic function to a coronal section of the palate. Three studies examined the effect of palate doming on /s/ variability. Brunner et al., (2009) examined variability in EPG contact patterns and found that speakers with low domed palates used little articulatory variability in target EPG pattern for /s/, whereas some with high domes had large variability. Yunusova et al., (2012) used EMA to measure variability in tongue height during consonants. They also found that subjects with low domed palates had less variability than those with high domed palates. Bakst (2016), in a PCA analysis of ultrasound images, also found that subjects with low-domed palates had less articulatory variability in /s/ than those with high-domed palates. These studies did statistically analyze apical vs laminal effects. The present study will consider only midline palate shape, that is, how the slope and convexity of the anterior midline palate influence the shape of the anterior tongue and the choice of apical versus laminal /s/.

Magnetic Resonance Imaging.

Magnetic Resonance Imaging (MRI) uses a strong magnetic field and radio frequency excitations to image various properties of the hydrogen atoms in tissue (cf. Brown, et al., 2014). Soft tissue has a high water content, so MRI is a highly useful and minimally invasive technique to study soft tissue anatomy (cf. Stone et al., 2018). Cine-MRI (as in cinema) can be used to capture the dynamic movements of subjects' tongues while performing speech tasks, enabling morphological characterization at the instant the /s/ sound is generated. Cine-MRI captures image information over several minutes while the subject repeats the task, and this information is pieced together to create a movie that represents a single execution of the task. Cine-MRI yields lower spatial resolution than that of anatomical MRI, which is captured while the subject lies still for several minutes. However, movies generated by cine-MRI have sufficient spatial resolution to allow clear visualization and measurement of the midline tongue surface (see Figure 1).

Curvature.

Most studies categorize /s/ production using visual inspection of data. Human raters attempt to distinguish between the two /s/-types by observing the midsagittal tongue profile (see Figure 1). The present study aimed to validate this type of categorization with a more objective measure of /s/-type, namely the curvature of the anterior midline tongue. Human ratings of /s/-type were used to test four curvature-based metrics that represent local and global tongue shape properties.

The curvature value, κ, represents the degree of deviation from a straight line at a point within a series of points (Casey, 1996). Here, the local curvature can be positive (i.e., arched or convex), zero (i.e., flat), or negative (i.e., depressed or concave). The midsagittal tongue profile in its entirety is naturally arched, or convex, at rest reflecting the curve of the vocal tract. Elevation of the tongue tip will reduce that convexity locally, more than elevation of the blade. Therefore, this study expected laminal /s/ to have a convex anterior tongue profile, because the blade is elevated by the body towards the alveolar ridge. For apical /s/, the anterior tongue profile was expected to be flatter or even concave, because the tongue tip is elevated to a greater extent than the tongue body.

Figure 1 about here

Two hypotheses were proposed. First, curvatures for apical /s/ were expected to be higher-dimensional than those for laminal /s/ due to a local flatness or concavity in the anterior tongue for apical /s/. Second, we expected that steeper palate slopes and a more protruded (convex) alveolar ridge region, would result in apical tongue shapes, with a less high tongue body, to properly funnel the air into the constriction.

MATERIALS AND METHODS

Subjects

Participants for this study were twenty healthy, native speakers of American English, who spoke with a Maryland regional accent. They were chosen from a larger database containing MRI and dental data and many have been used in previous studies, such as Stone, et al., (2013) and Grimm, et al., (2017). The subjects had normal hearing test results, including acuity, word recognition tests, and speech reception thresholds. The subjects had an average age of 35.8 years (SD=12) and included 9 males and 11 females (n=20).

Speech task

The speech task was /əsuk/ (“a souk”). This task was chosen for several reasons. First, it begins with a fairly neutral tongue position (schwa), and after the forward movement into /s/ the tongue motion is in a straightforward backward/upward direction. Second, the high vowel minimizes jaw motion, maximizing the deformation of the tongue when creating the sounds. Finally, the cine image acquisition was limited to 1 second to allow comparison between these data and tagged data collected in the same session (not used in this study). For these subjects there was a distribution of /s/-types, with 12 apical and 8 laminal speakers (see Figure 2). Categorization of apical or laminal /s/ for each subject was done independently by a speech scientist and two dentists trained by the speech scientist. The time-frame in which the tongue-palate constriction first appeared for /s/ was chosen for measurement. The three raters used visual inspection criteria consistent with Dart (1991, p. 12), who used the terms to refer to the part of the tongue used to make the constriction. Apical refers to the tip, and laminal to the blade. Disagreement by one rater was addressed by consultation among all three.

Figure 2 about here

Data Collection and Measurements

Cine-MRI.

MRI data were acquired on a 3 Tesla Tim Trio scanner (Siemens Healthcare, Erlangen, Germany), with a 12-channel head coil and a 4-channel neck coil. Cine MRI was acquired using a segmented gradient echo sequence at an in-plane resolution of 1.875

mm/pixel, field of view (FOV) of 240 mm×240 mm slice, thickness of 6 mm, TE of 1.33 ms, and TR of 2 seconds. Five speech repetitions were used to complete data acquisition for each single slice including 26 time frames of 38 ms each. Cine-MRI creates a single movie by ensemble summation of multiple repetitions of the speech task. Each time frame (1–26) is averaged with the same time frame from all five repetitions to boost signal strength because the signal emitted by the hydrogen protons in the short time frame is quite weak. The cine-MRI recordings were made during a 1 s recording period within a 2 s repeat cycle. Data were collected at multiple slices and in three orientations (sagittal, coronal, and axial). The mid-sagittal slice was identified based on all three datasets, and used for the tongue analysis in this study. Subjects were trained to speak the words to a 4-beat metronome to increase the precision of repetitions, using the methods of Masaki et al., (1999).

High resolution MRI volumes for each subject were collected in the same session as the cine-MRI data and in the same orientation, so that the two data sets could be overlaid (cf. Stone, et al., 2013). These volumes were used to identify the location of the anterior edge (alveolar) of the first molar tooth roots, which along with the mid-palate point at the same location, formed a plane perpendicular to the occlusal plane. This plane served as a landmark for placing the 5th midsagittal tongue surface point during the /s/.

Dental cast.

Dental casts were available for all subjects collected from alginate impressions and poured in dental stone. Subjects were not included if they were missing first molars, had a significant palatal torus, or if the cast had major imperfections that made palatal measurements inaccurate. The acceptable casts were scanned using a 3D optical scanner (Ortho Insight 3D Scanner, Motion View Software, 2016). Three landmarks were measured on both the stone and digital dental casts (see Figure 3a). These three material points and the occlusal plane were used to calculate the convexity angle and the slope of the anterior palate. The stone casts were measured by hand using dial calipers. The digital casts were measured using MeshLab V1.3.3 (Cignoni et al., 2008). Those digital and stone cast values that did not agree were remeasured. Once the digital points were accurately identified, the 3-dimensional coordinates were exported to an Excel spreadsheet (Microsoft, Seattle, USA) file for analysis. The two palate angles were calculated as follows:

1. Convexity Angle (CA): This angle quantifies the prominence of the alveolar ridge of the hard palate. The CA is formed by an angle formed by points 1, 2, 3 in Figure 3, a and b. These points represent the central incisor interdental papilla (point 1), the base of the incisive papilla (point 2) , and the palate high-point adjacent to the first molars (point 3), shown as black dotted lines (Figure 3b). The incisive papilla is a small oval protruberance that sits on the incisive foramen directly behind the central incisor teeth. As it is a protuberance, the CA is always slightly convex. The subjects were divided into two groups based on the range of their convexity angles, which was 147º to 177º. Higher numbers indicate flatter, less convex shapes, because 180º is flat (colinear points). Low convexity angles were defined as ≤ 173º, which was the median value.

2. Anterior Angle (AA): The AA is at point 0, and is formed by the projection of a line (dashed green) drawn between the base of the incisive papilla (point 2) and the interdental papilla (point 1) at the intersection with the occlusal plane (point 0). The perpendicular from the occlusal plane to the base of the incisive papilla (Figure 3b, vertical green line) completes the triangle. The anterior angle represents the slope of the anterior midline palate. Subjects were sorted into two AA Groups, where low angles were $\leq 37.0^{o}$, which was the median angle of our larger database.

Figure 3 about here.

Tongue curvature measures.

Tongue profile point sequence: The midline tongue profile was identified in the time-frame identified as the maximum constriction for /s/. Eight roughly equidistant tissue points were selected as xy coordinates. Five were between the tongue tip and the first molar, and three were posterior to the first molar. In order to normalize points across subjects the following method was used. Point 1 was the most anterior point on the upper profile of the tongue. Point 5 was selected at the plane cut by the M1 roots onto the profile of the midsagittal tongue (see Figure 3c). To make this projection, a vertical plane was defined at M1 by selecting 3 points—one at each M1 alveolus and a third point at the midpoint of the palate at the M1 alveolus. These 3 points defined a plane perpendicular to the occlusal plane, which cuts through the tongue coronally at the first molar (Grimm et al., 2017). Points 2, 3, and 4 were selected manually to be equidistant visually between points 1 and 5. The first 5 points covered the region of the tongue tip and blade. Since human observers may use more than just the tip and blade in making their decision, points 6–8 were selected posterior to point 5 using the same manual selection of spacing as the first 5 points. This allowed a larger shape region to be considered objectively.

Basic Curvature calculation: The resulting sequence of 8 points was considered to be part of a curve on which κ (curvature) was calculated by fitting a circle to every 3 consecutive points (κ was not defined at the endpoints). We approximated *local* values of κ by fitting a circle of radius r passing through 3 adjacent Cartesian points in the sequence described above (Cassey, 1996). For 3 such points (say, p1, p2, and p3), $\kappa = r^{-1}$ at the center point can be extracted from

$$r = \frac{1}{2}\frac{||v_{12}||||v_{13}||||v_{32}||}{||v_{\mathrm{axis}}||}, \tag{1}$$

where $\boldsymbol{v}_{12}$, $\boldsymbol{v}_{13}$, and $\boldsymbol{v}_{23}$ are vectors between the points, and $\boldsymbol{v}_{axis} = \boldsymbol{v}_{12} \times \boldsymbol{v}_{32}$ is normal to the plane in which the circle is defined. Curvature calculations were implemented in a script written in MATLAB v2015a (Natick, MA, USA). Curvature values were assigned a sign to represent whether the local shape acted with or against the global convexity of all points along the tongue profile. Figure 4 shows the global curvature represented as a dotted circle with radius R, which has been fitted to the points in the 8-point sequence using least squares (Gander, 1994). The direction of the global convexity is represented by the vector from each point in the sequence towards the center of the circle (C) associated with R. Likewise, the local curve shape is represented by the vector from each point to the center of the local circle (c) associated with r (solid blue or solid red). Thus, κ was negative if the angle between the vectors (C,P,c) was greater than 90° (Figure 4, point 3), and positive if the angle was less than 90° (point 7).

Figure 4 about here.

Profile shape classification: As a reference, apical and laminal /s/ were identified from the images by visual inspection as described above. For quantification, four data-driven approaches were also used to classify the shapes based on the 8 point sequence. Because the data points are coarse, several mm apart, some of the methods below include normalization of subject size as well as refinement by adding more points.

1. Minimum Curvature (MC). This method uses the minimum local curvature value among the measured points, be it a small convex or a large concave curve. Negative values of κ represent a local concavity in the overall curvature. Using this approach, the lowest curvature values during /s/ typically occurred at points 3, 4 or 5, so the lowest of these three values was selected to represent the anterior tongue shape for the /s/ of that subject. (The concept is illustrated in Figure 5, row 1.) This is the only one of the methods that used the sign of the curvature and is fairly intuitive in reflecting concave versus convex minima.

2. Averaged Largest Curvatures (ALC). The ALC method consists of classifying profile shapes based on the largest curvature values (or smallest r circles), to capture deviations from the smooth arc formed by the anterior tongue profile (as shown in Figure 5, row 2). It is not sign sensitive. The two largest curvature values were averaged together because the addition of a second anatomical region increases sensitivity to the complexity of the profile curve. The largest curvature values are examined irrespective of sign, and thus do not contain zero values. This prevents flat surfaces of the tongue from dominating the classification results. Flat surface regions can occur locally in both apical and laminal /s/ shapes.

3. Normalized ALC (NALC). To account for size differences between subjects, the ALC method was normalized using the global curvature. The ALC was inverted to approximate a radius, which was then divided by the size normalization factor, R (see Figure 5, row 3). As with ALC, this approach captures the complexity of the curve, and includes normalization as well as averaging.

4. NALC with Interpolation (NALCi). This method consisted of recalculating NALC after refining the point sequence by interpolating 10 additional points between each original point via a cubic spline. This method determines whether point distance is important when calculating curvature. The use of 78 points instead of 8 enables a better approximation of local curvatures. The length scale differs for each subject based on the size and spacing of their teeth; tissue point 5 is located at the first molar. To maintain sensitivity to the length scale, the top 20 local curvatures or 1/4th of the curvature measurements were averaged instead of the top 2 as in NALC.

Figure 5 about here.

The presented approaches are intended to balance efficacy and conceptual accessibility based on our experience. However, the list of methods described above is by no means exhaustive, and there are multiple plausible shape classification schemes. For instance, it is possible to approximate the properties of a continuous curve (including rotation, axial torsion, and cumulative curvature through a line integral) as has been demonstrated to classify shape differences in the spine (Donzelli, 2015), or to measure diversity of curvature via the standard deviation of local curvature values.

Statistical Analyses

Mystat 12 (Systat Software, San Jose, CA) was used to calculate statistics on these data. Because of the small amount of data, non-parametric statistics were used. First, a Spearman's Rho correlation (Myers and Well, 2003) was performed between AA and CA, to determine whether the two palate measurements were independent of each other (see Figure 6). They were found to be uncorrelated (rho=0.005). A rho of 2.11 was needed for significance at p=0.05 given the number of subjects in the study. Therefore, the two palate angles were treated independently in subsequent analyses.

Figure 6 about here.

Curvature was grouped separately by /s/-type, AA, and CA, and the median differences tested with two-tailed Mann-Whitney U tests.

RESULTS

We hypothesized that the curvature-based metrics would classify the anterior tongue profile into categories of apical and laminal /s/ consistent with the subjective classification of three raters. To test this, the four curvature quantities, MC, ALC, NALC, and NALCi, were compared to the apical and laminal subjectively rated groups.

The metric classification results appear in Table 1 and are visualized in Figures 7 and 8. The MC method did not show a significant difference between the apical and laminal shape categories (U = 26, p = 0.09) (see Figures 7 and 8). However, the ALC analysis without normalization also did not show a significant difference between the apical and laminal shape categories (U = 55, p = 0.589) (Figures 7 and 8).

The third measure, the NALC, resulted in a statistically significant differentiation between /s/ types (U = 16, p = 0.028). The NALC, which measures the ratio between the averaged largest curvatures and the global curvature, found that the laminal curvatures were more similar to the global curvatures than were the apical ones, that is, the ratio was closer to 1. The laminal profiles had a median ratio of 0.368 ± 0.14 and the apical median was 0.225 ± 0.10 (Figures 7 and 8). This means that the apical tongue had a less convex shape, often containing an anterior local concavity. Thus, this metric captured somewhat more complexity in the apical than the laminal /s/.

The final metric, NALCi, was also statistically different between groups ($U=15$, $p=0.028$). The laminal profiles had a median value of 0.260 ± 0.10 for, and the apical profile shapes averaged 0.158 ± 0.07 (see Figures 7 and 8). A correlation showed that NALC and NALCi were highly correlated ($R=0.99$).

Figure 7-8 about here.

Table 1 about here

In addition to the /s/-type effect, this study examined the effect of palate shape and slope on curvature. Mann Whitney U tests found that palate convexity angle (CA) had no significant effect on curvature. The anterior angle (AA), however, did have a significant effect on tongue shape for NALC ($U = 16$, $p = 0.019$). Less steep anterior palate slopes were more likely to produce an apical /s/. AA was close to significant, with identical U and p values, for MC ($U = 21$, $p = 0.052$), and NALCi ($U= 21$, $p=0.052$).

DISCUSSION

Apical-Laminal Effect on Curvature

The main goal of this study was to use curvature to capture quantitatively apical and laminal /s/ shapes in the midsagittal tongue. Within even a single tongue profile there is variability in curvature between the tip and the region beyond the first molar, as measured in this study. In addition, vocal tract size differs across subjects, so scaling becomes an issue in quantification of shape. Visual inspection suggested that a laminal /s/ was associated with a convex-to-flat tongue profile shape, while apical /s/ was associated with a flat-to-concave shape. Only the MC used signs when calculating curvature; the other three methods examined only curvature magnitude. Results showed that using the normalized curvature quantities, NALC and NALCi, the subjective categories of apical and laminal /s/ predicted the shape of the anterior tongue very well (Figure 5, Table 1). The apical /s/ shape was slightly more complex than the laminal /s/, with more zero crossings. Every time the curvature value passes through zero and switches sign, an inflection point occurs. More inflection points create more curvature minima. If the curvatures of the apical and laminal tongues had been mirror images, this method would not work; however, they were not. Thus, one outcome of this study was the observation that apical tongue contours have more shape complexity than laminal ones.

Metric Representation of Tongue Curvature

The second goal of this study was to optimize the curvature metric used to represent the midsagittal tongue profile. The simplest metric was the MC value as it identified the local tongue tip shape. However, an MC value near zero occurred in 1/2 of the subjects, and in both apical and laminal /s/ shapes (Figure 6). A value of zero arises when points are colinear, which can be a feature of the profile or from the digital nature of the images in cases where three consecutive points lay in the same (or close to the same) voxel row, resulting in a radius of curvature approaching infinity. For these subjects especially, it was clear that a larger region of the tongue needed to be used in quantifying its shape. The second metric, ALC, indicated that the radius of the smallest circles (largest local curvature) in the laminal /s/ profiles could be close in magnitude to the circle encompassing all points in the sequence (Figures 4 and 5). This was generally not the case for the shape of apical /s/ profiles, because the local circle fits were generally smaller than the global circle fit. However, this metric also failed to distinguish the shape categories. The third metric, NALC, included a normalization factor (the global radius of curvature), which prevented tongue size differences from affecting curvature values. Cases such as that shown in Figure 5 also suggest that apical profiles may have a larger radius of global curvature; thus, the numerator would decrease while the denominator increases, magnifying the sensitivity of the metric. The NALC clearly distinguished between the two groups of tongue shapes in a manner consistent with the raters' categorizations. The similarity of results between the NALC and the fourth metric, NALCi, indicated that the addition of interpolated points was less important than normalizing the length scale used in the analysis (Figures 9, 10). Thus, the automated, data-driven metrics showed that the human /s/ shape categories appeared to follow curvature differences in the anterior tongue, in which apical /s/ had a more complex shape with a local flat or convex region.

It can be observed that subject 18 (S-18) was unusual. In Figure 6, S-18 was the outlier who had the least upwardly sloped and the most convexly shaped palate of all the subjects. S-18 also was physically a large person, with a large oral cavity and tongue. Although S-18 was judged to have a laminal tongue shape, (Figure 2, subj 18), the tip region was very flat, and not inconsistent with the apical shapes. The MC and ALC methods put 18 in the middle reflecting the ambiguous shape. By dividing the largest curvatures by the global curvature, the NALC and NALCi eliminated the effects of the large tongue size by using a ratio, but that also removed the shape ambiguity in the quantity. Instead, the large normalized circles used to comprise NALC and NALCi placed S-18 numerically in the apical region.

Palate Effects on Curvature.

This paper hypothesized that anterior palate shape might affect anterior tongue profile shape. The effect of CA on tongue shape was non-significant for all four metrics. However, the AA had a significant effect on NALC ($p = 0.019$), and approached significance for MC ($p = 0.052$) and NALCi ($p = 0.052$). Flatter anterior palate slopes were more likely to produce an apical /s/ and steeper ones led to laminal /s/. This was of interest as our previous research (Grimm et al., 2017) showed that palate height affected the /s/-type categorization made by human raters. These two results are consistent, because even though palate height does not correlate with AA, there is a tendency for a steep AA to accompany a higher palate (Grimm, et al., 2017).

CONCLUSIONS

This study found objective curvature measures of the midsagittal tongue, when scaled across subjects, supported the classical, visually-determined categories of apical and laminal /s/. More convex tongue shapes were associated with the laminal /s/ and occurred with steeper palate slopes. The flatter anterior palates, associated with the apical /s/, sometimes produced concave regions in the anterior tongue, and occasionally more complex profile shapes (more zero crossings). It is tempting to think that differences between these two /s/-types is entirely due to morphology of the palate. However, glossectomy patients tend to use laminal /s/ irrespective of palate features, due to difficulty controlling the tongue tip (Grimm et al., 2017). Thus, palatal constraints are not obligatory.

In our experience, the best metric was the Normalized Averaged Largest Curvatures (NALC). Both NALC and NALCi included a normalization factor, which allowed them to distinguish between the two /s/ types and also show the relationship between tongue shape and palate angle. However, NALC is more convenient and cost effective than NALCi because it does not require interpolation of additional points, The NALC prevented tongue size differences from affecting curvature values and obscuring subject differences.

ACKNOWLEDGMENTS

The authors would like to thank Susan Rizk, Nada Al Shehry and Jun Hwang for their assistance in the data analysis. This research was supported by NIH grants R01 CA133015 (PI: M. Stone) and R01 DC014747 (PI: J. Prince).

REFERENCES

Bakst, S. (2016) “Differences in the relationship between palate shape, articulation, and acoustics of American English /r/ and /s/.” UC Berkeley Phonetics and Phonology Lab Annual Report (2016)

Brown, R. W., Haacke, E. M., Cheng, Y. C. N., Thompson, M. R., & Venkatesan, R. (2014). “Magnetic resonance imaging: physical principles and sequence design.” 2nd Edition. John Wiley & Sons.

Brunner, J., Fuchs, S., and Perrier, P. (2009) “On the relationship between palate shape and articulatory behavior.” Journal of the Acoustical Society of America 125, 3936-3949.

Cassey, J. (1996) “Exploring curvature.” 1st Edition. Springer.

Cignoni, P., Callieri, M., Corsini, M., Dellepiane, M., Ganovelli, F., & Ranzuglia, G. (2008). Sixth Eurographics Italian Chapter Conference. Salerno, Italy, 129-136.

Dart, S.N. (1991). “Articulatory and acoustic properties of apical and laminal articulations.” UCLA Working Papers in Phonetics, No. 79

Dart, S.N. (1998) “Comparing French and English coronal consonant articulation.” J. Phonetics. 26, 71-94

Donzelli S., Poma S., Balzarini L., Borboni A., Respizzi S., Villafane J. H., Fabio Zaina F., and Negrini S. (2015) “State of the art of current 3-D scoliosis classifications: a systematic review from a clinical perspective.” J. of NeuroEngineering and Rehabilitation vol. 12 no. 91

Gander W., Golub G. H., Strebel R. (1994) “Least-squares fitting of circles and ellipses.” BIT Numerical Mathematics vol. 34 pp. 558-578

Grimm, D, Stone, M, Woo, J, Lee, J, Hwang, J-H, Bedrosian, GE and Prince, JL. (2017) The effects of palate features and glossectomy surgery on /s/ production. Journal of Speech, Language, Hearing Research. vol 60, pp. 3417-3425. https://doi.org/10.1044/2017_JSLHR-S-16-0425

Icht, M and Ben David, B (2018) “Sibilant production in Hebrew-speaking adults: Apical versus laminal.” Clinical Linguistics & Phonetics. vol 32 no. 3: 193-212.

Myers, Jerome L.; Well, Arnold D. (2003). Research Design and Statistical Analysis (2nd ed.). Lawrence Erlbaum. p. 508.

Narayanan, S. S., Alwan, A. A., and Haker, K. (1995). "An articulatory study of fricative consonants using magnetic resonance imaging," J. Acoust. Soc. Am. 93, 1325–1335

Reichard, R., Stone, M, Woo, J, Romberg, E, Murano, EZ, Prince, JL (2012) Motion of apical and laminal /s/ in normal and post-glossectomy speakers. Proceedings of Acoustics 2012, May 14-18, 2012, Hong Kong, China. of the Oral Tongue." Oral Oncol, 49(11): 1083–1087.

Stone, M., Rizk, S., Woo, J, Murano, E.Z., Chen, H., Prince, J.L., (2013), "Frequency of apical and laminal /s/ in normal and post-glossectomy patients." Journal of Medical Speech Language Pathology. 20(4):106-111.

Stone, M, Woo, J, Lee, J, Poole, T, Seagraves, A, Chung, M, Kim, E, Murano, EZ, Prince, JL & Blemker, SS.(2018) Structure and variability in human tongue muscle anatomy, Computer Methods in Biomechanics and Biomedical Engineering: Imaging & Visualization, 6:5, 499-507.

Stoner, R., Gateley, G., & Rivers, D. (1987). “An investigation of apical and dorsal /s/ production.” Texas Journal of Audiology and Speech Pathology, XIII(2), 40-42.

Yunusova, Y., Rosenthal, J.S., Rudy, K., Baljko, M., Daskalogiannakis, J. (2012) “Positional targets for lingual consonants defined using electromagnetic articulography.” J. Acoust. Soc. Am. 132(2): 1027–1038.

TABLE 1. Median values of curvature in Apical and Laminal groups.

	Apical	Laminal	*p*-value
MC	-0.020 ± 0.02	-0.010 ± 0.02	0.090
ALC	0.062 ± 0.02	0.057 ± 0.01	0.589
NALC	0.225 ± 0.10	0.368 ± 0.14	0.028*
NALCi	0.158 ± 0.07	0.260 ± 0.10	0.028*

FIGURE CAPTIONS

Figure 1. Mid-sagittal MRI images of apical (left) and laminal (right) /s/.

Figure 2. Twenty midline tongue profiles showing apical and laminal shapes.

Figure 3. Measurement points selected on (a) the palate cast, (b) the midsagittal palate profile, and (c) the tongue surface. Palate points are (1) the interdental papilla between incisors, (2) the base of the incisive papilla, (3) the deepest point of the palate adjacent to the first molars. The eight tongue points include 2 landmarks: (1) the tongue tip, (5) the anterior edge of the first molars. Tongue points are equidistant.

Figure 4 Curvature calculation and sign assignment in discrete points. The global circle (dotted line) fit to all eight points, has a radius R and is centered at C. Local curvature values are extracted by fitting a circle on 3 neighboring points. The local circle has a radius r and is centered at c. The global fit is used to determine the sign of the local curvature values. A negative sign is assigned when the internal angle in the segment cpC is larger than 90° (blue), and positive if the angle is smaller than 90° (red).

Figure 5. Strategies for numerical distinction between apical and laminal profile shapes. Top row: the minimum curvature method (MC) places emphasis on curvatures with relatively large negative values (left), and values close to zero (right). Second row: the average largest curvature method (ALC) averages the 2 largest curvature values (dotted, solid) in the tongue profile. Smaller circles yield larger averaged curvature values and typically reflect apical shapes (left). Third row: the normalized ALC method (NALC) is the ratio of the ALC divided by the global curvature (aqua), which normalizes for size differences among subjects. Laminal tongue profiles have ratios closer to 1 (right). Bottom row: the NALC with interpolated points method (NALCi) is applied to a more continuous (interpolated) curve to assess the effects of closer points. Note that in NALCi, the interpolated points are close together and give the impression of a continuous line.

Figure 6. Scatterplot of the Convexity Angle and the Anterior Angle of the Palate.

Figure 7: Group comparison per different shape classification metrics. MSC and ALC are curvature measurements with units as noted, NALC and NALCi are both normalized curvature radii ratios (the mark (-) denotes a dimensionless quantity). Significance is indicated with an asterisk, which indicates $p<0.05$.

Figure 8. Ranked shape classification metrics. The metric value for each participant was ranked in ascending order along the x-axis.

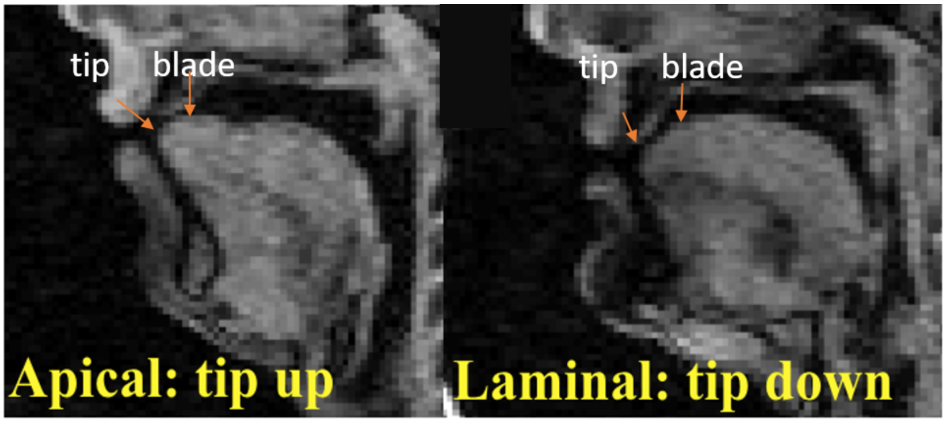

Mid-sagittal MRI images of apical (left) and laminal (right) /s/.

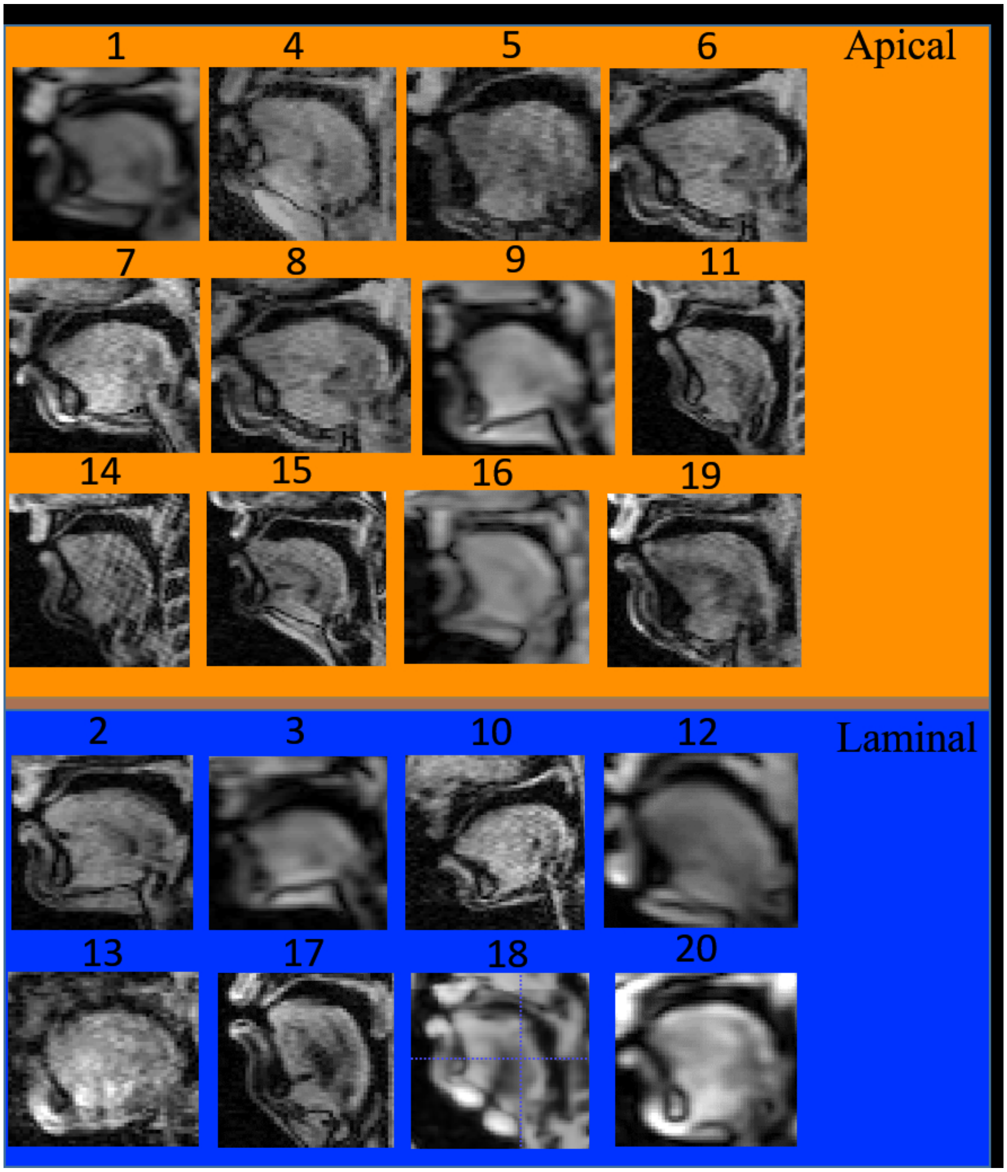

Figure 2. Twenty midline tongue profiles showing apical and laminal shapes.

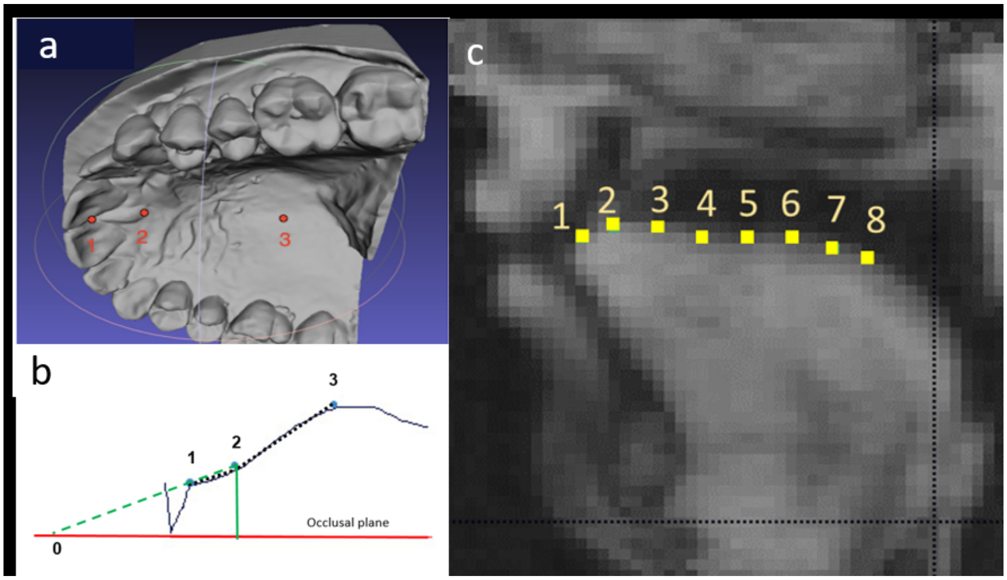

Measurement points selected on (a) the palate cast, (b) the midsagittal palate profile, and (c) the tongue surface. Palate points are (1) the interdental papilla between incisors, (2) the base of the incisive papilla, (3) the deepest point of the palate adjacent to the first molars. The eight tongue points include 2 landmarks: (1) the tongue tip, (5) the anterior edge of the first molars. Tongue points are equidistant.

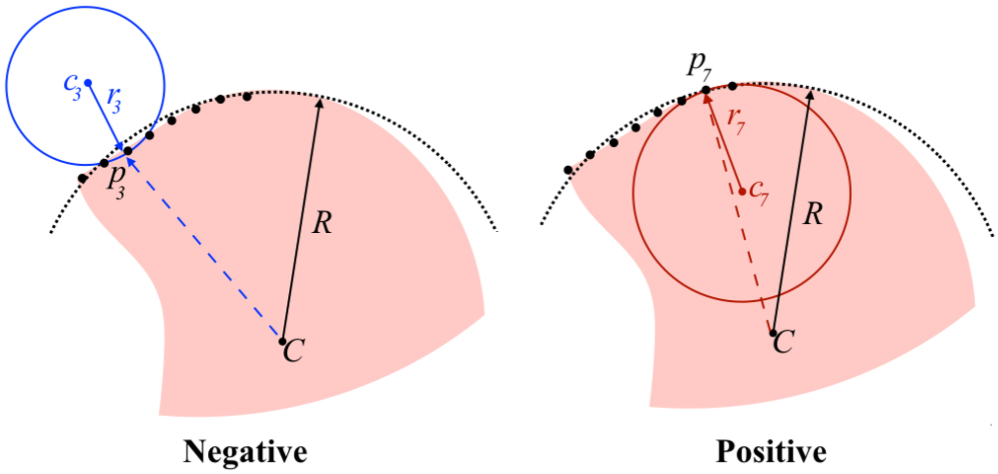

Curvature calculation and sign assignment in discrete points. The global circle (dotted line) fit to all eight points, has a radius R and is centered at C. Local curvature values are extracted by fitting a circle on 3 neighboring points. The local circle has a radius r and is centered at c. The global fit is used to determine the sign of the local curvature values. A negative sign is assigned when the internal angle in the segment cpC is larger than 90° (blue), and positive if the angle is smaller than 90° (red).

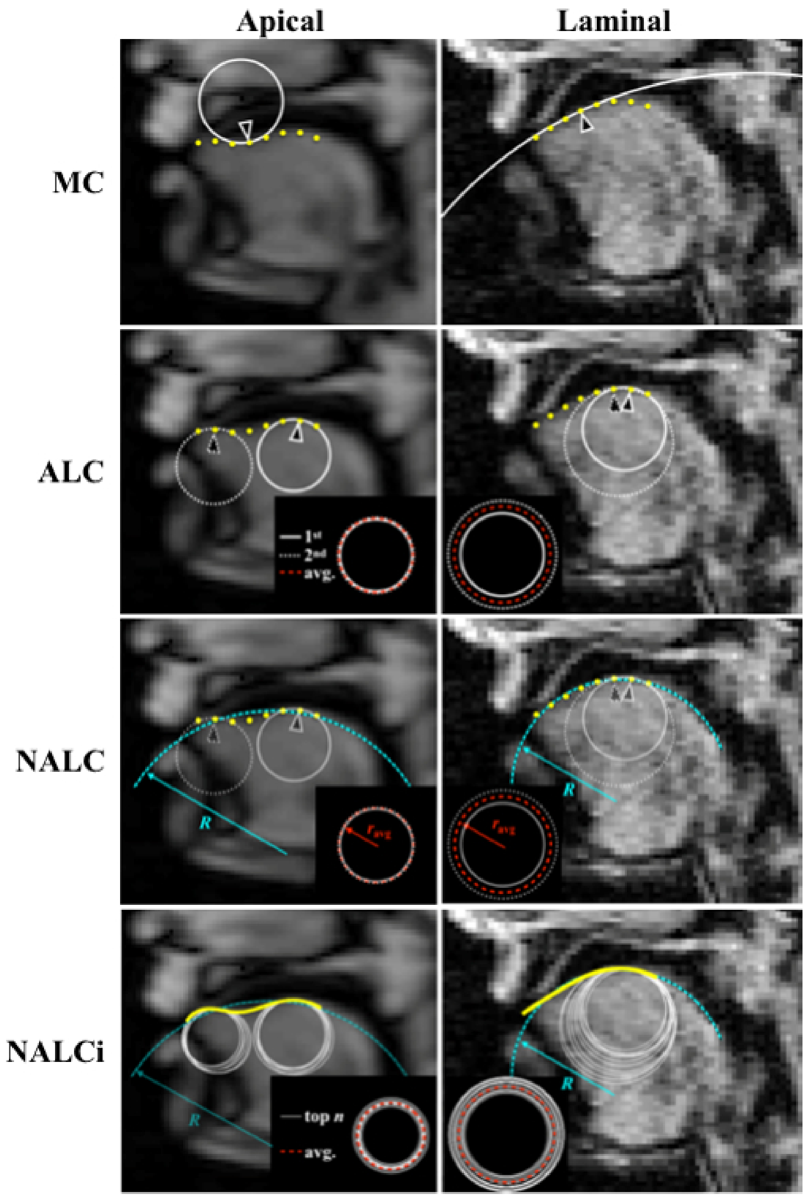

Strategies for numerical distinction between apical and laminal profile shapes. Top row: the minimum curvature method (MC) places emphasis on curvatures with relatively large negative values (left), and values close to zero (right). Second row: the average largest curvature method (ALC) averages the 2 largest curvature values (dotted, solid) in the tongue profile. Smaller circles yield larger averaged curvature values and typically reflect apical shapes (left). Third row: the normalized ALC method (NALC) is the ratio of the ALC divided by the global curvature (aqua), which normalizes for size differences among subjects. Laminal tongue profiles have ratios closer to 1 (right). Bottom row: the NALC with interpolated points method (NALCi) is applied to a more continuous (interpolated) curve to assess the effects of closer points. Note that in NALCi, the interpolated points are close together and give the impression of a continuous line.

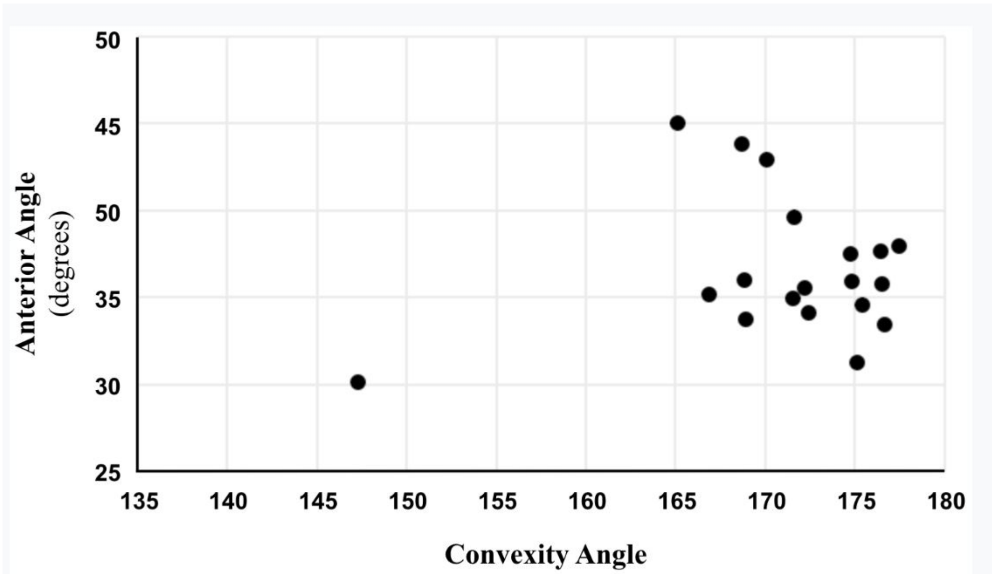

Figure 6. Scatterplot of the Convexity Angle and the Anterior Angle of the Palate.

242x139mm (120 x 120 DPI)

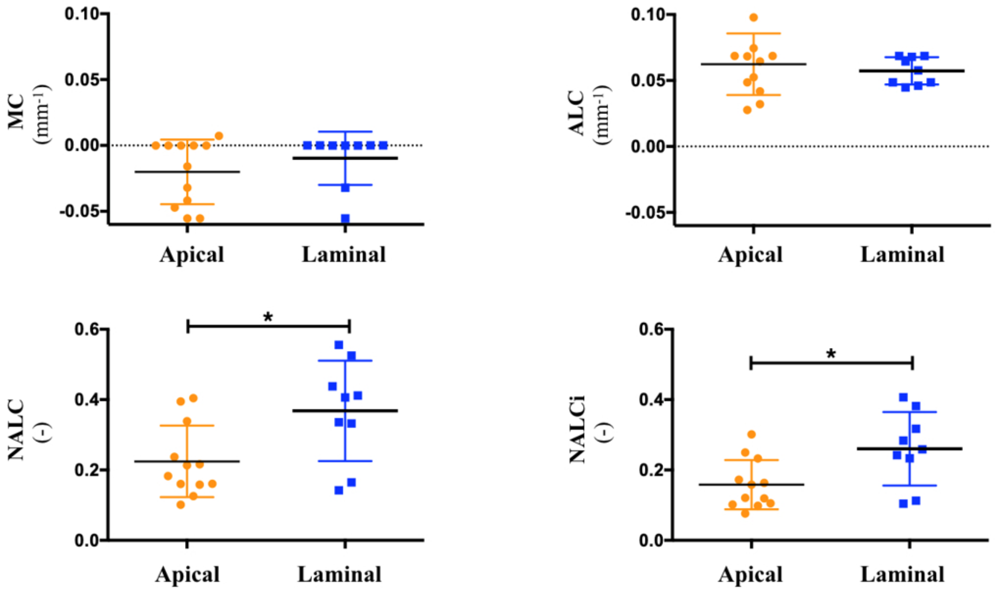

Group comparison per different shape classification metrics. MSC and ALC are curvature measurements with units as noted, NALC and NALCi are both normalized curvature radii ratios (the mark (-) denotes a dimensionless quantity). Significance is indicated with an asterisk, which indicates p<0.05.

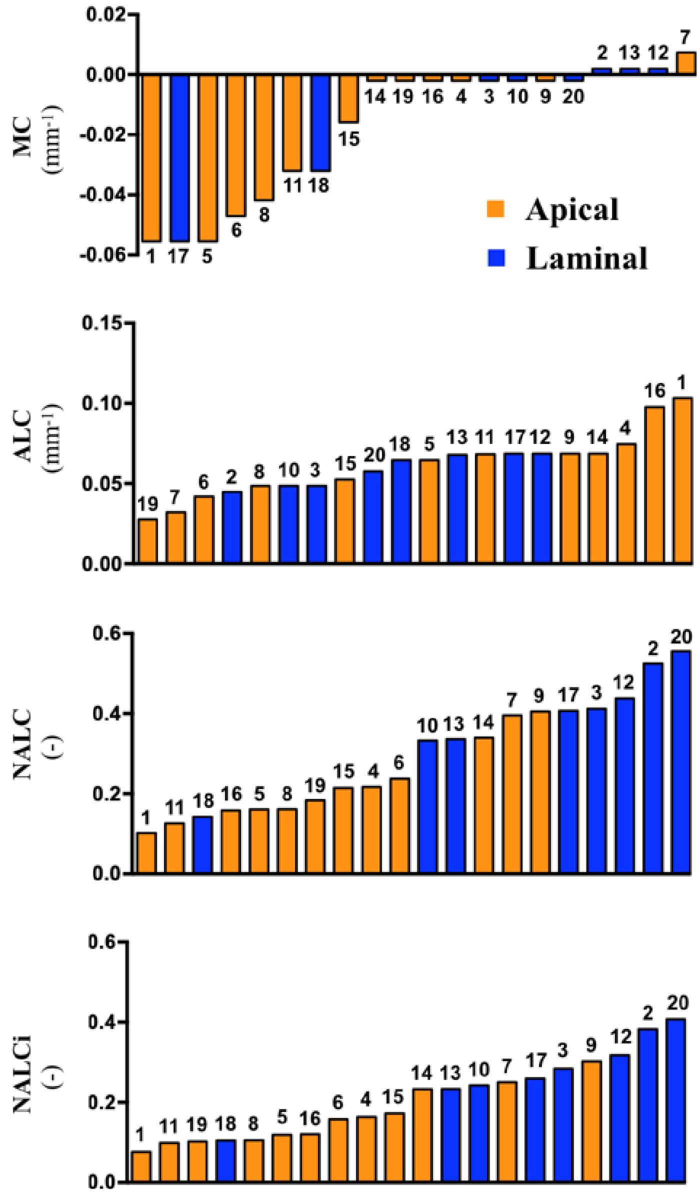

Ranked shape classification metrics. The metric value for each participant was ranked in ascending order along the x-axis.

Points for curvature calculation

Subj1		X	Y	Z	Label #	Group 1
	1	5.9175	114.0108	-7.743	25	
	2	6.1656	112.1026	-2.1347	25	
	3	5.7619	106.4902	-0.2653	25	
	4	5.0322	99.0258	-0.2653	25	
	5	4.485	93.4275	-0.2653	25	
	6	4.0813	87.8152	1.6042	25	
	7	3.6776	82.2028	3.4736	25	
	8	3.1304	76.6045	3.4736	25	

Subj2		X	Y	Z	Label #	Group 2
	1	25.681	111.2054	-3.8185	25	
	2	25.2381	107.4759	-0.0741	25	
	3	24.4728	101.8995	3.6703	25	
	4	23.6064	96.3407	5.5425	25	
	5	22.4174	88.9348	7.4147	25	
	6	21.1273	81.5466	7.4147	25	
	7	19.8372	74.1584	7.4147	25	
	8	18.7686	68.6349	5.5425	25	

Subj3		X	Y	Z	Label #	Group 2
	1	2.3884	100.1524	7.0385	25	
	2	2.4052	94.5214	10.7794	25	
	3	2.2915	88.896	12.6498	25	
	4	2.1779	83.2706	14.5203	25	
	5	1.983	75.772	16.3907	25	
	6	1.7389	70.1523	16.3907	25	
	7	1.4949	64.5326	16.3907	25	
	8	1.1205	58.9186	14.5203	25	

Subj4		X	Y	Z	Label #	Group 1
	1	4.6617	106.3828	11.0258	25	
	2	4.2532	100.7725	12.9003	25	
	3	3.8448	95.1622	14.7748	25	
	4	3.3937	89.5553	14.7748	25	
	5	2.9426	83.9484	14.7749	25	
	6	2.4916	78.3415	14.7749	25	
	7	2.0405	72.7346	14.7749	25	
	8	1.6972	69.0001	12.9003	25	

subj5		X	Y	Z	Label #	Group 1
	1	-0.8568	100.0548	8.0326	25	
	2	-0.5715	96.3041	11.771	25	
	3	-0.291	90.6784	15.5094	25	
	4	-0.3103	83.1784	15.5094	25	
	5	-0.3248	77.5534	15.5094	25	
	6	-0.1918	71.928	17.3785	25	
	7	-0.0589	66.3027	19.2477	25	
	8	-0.0782	58.8027	19.2477	25	

subj6		X	Y	Z	Label #	Group 1

	1	9.5831	106.8027	7.3474	25	
	2	9.2659	101.1865	9.2219	25	
	3	8.8571	93.6975	11.0964	25	
	4	8.4483	86.2086	12.9709	25	
	5	8.0885	80.5944	16.72	25	
	6	7.6797	73.1055	18.5945	25	
	7	7.4051	67.4872	18.5945	25	
	8	7.0814	59.994	16.72	25	
subj7		X	Y	Z	Label #	Group 1
	1	3.1191	111.62	2.3895	25	
	2	2.9092	105.9988	4.2643	25	
	3	2.7254	100.3766	8.0139	25	
	4	2.4629	92.881	11.7635	25	
	5	2.1217	83.5121	15.5132	25	
	6	1.9118	77.8909	17.388	25	
	7	1.597	70.3975	17.388	25	
	8	1.3609	64.7775	17.388	25	
subj8		X	Y	Z	Label #	Group 1
	1	6.9592	108.8322	2.8759	25	
	2	6.7816	103.2091	6.6247	25	
	3	6.5551	97.5885	8.499	25	
	4	6.3286	91.9678	10.3734	25	
	5	6.151	86.3448	14.1221	25	
	6	5.9245	80.7241	15.9965	25	
	7	5.698	75.1035	17.8708	25	
	8	5.4227	69.4852	17.8708	25	
subj9		X	Y	Z	Label #	Group 1
	1	9.5471	108.2146	3.941	25	
	2	9.3503	104.4695	7.6907	25	
	3	9.1535	100.7244	11.4405	25	
	4	8.8127	95.1097	13.3153	25	
	5	8.4719	89.495	15.1902	25	
	6	8.1083	83.8817	15.1902	25	
	7	7.7448	78.2685	15.1902	25	
	8	7.3812	72.6553	15.1902	25	
subj10		X	Y	Z	Label #	Group 2
	1	-7.2311	95.3171	2.5081	25	
	2	-6.6649	89.712	6.2452	25	
	3	-5.9431	84.114	11.8507	25	
	4	-5.3769	78.5089	15.5878	25	
	5	-4.8107	72.9038	19.3248	25	
	6	-4.4001	67.2917	21.1933	25	
	7	-3.9894	61.6795	23.0619	25	
	8	-3.7344	56.0603	23.0619	25	
subj11		X	Y	Z	Label #	Group 1
	1	-2.1266	103.6482	2.1829	25	
	2	-1.6955	98.0397	5.9327	25	

	3	-1.1724	90.5579	5.9327	25	
	4	-0.6685	83.0748	4.0578	25	
	5	-0.1454	75.5931	4.0578	25	
	6	0.247	69.9818	4.0578	25	
	7	0.6394	64.3705	4.0578	25	
	8	1.0124	58.7579	2.1829	25	
subj12		X	Y	Z	Label #	Group 2
	1	-5.2841	118.4122	-16.5033	25	
	2	-4.9357	114.6693	-12.7625	25	
	3	-4.5873	110.9263	-9.0217	25	
	4	-4.3268	105.3058	-7.1513	25	
	5	-4.0232	97.8108	-5.2809	25	
	6	-3.8938	92.1873	-5.2808	25	
	7	-3.7644	86.5638	-5.2808	25	
	8	-3.7661	80.9372	-7.1513	25	
subj13		X	Y	Z	Label #	Group 2
	1	7.8335	103.9016	-7.3036	25	
	2	7.64	100.1562	-1.6788	25	
	3	7.1879	92.6698	2.0711	25	
	4	6.8733	87.0534	7.6959	25	
	5	6.405	79.568	9.5708	25	
	6	5.9367	72.0826	11.4457	25	
	7	5.4522	64.5983	11.4457	25	
	8	4.9514	57.115	9.5708	25	
subj14		X	Y	Z	Label #	Group 1
	1	-0.5109	107.5101	5.4146	25	
	2	-0.2576	103.7674	9.1634	25	
	3	0.0248	98.1493	11.0377	25	
	4	0.356	92.5332	14.7865	25	
	5	0.6385	86.9151	16.6608	25	
	6	0.9209	81.297	18.5352	25	
	7	1.1546	75.6768	18.5352	25	
	8	1.3396	70.0547	16.6608	25	
subj15		X	Y	Z	Label #	Group 1
	1	8.4596	116.6077	0.289	25	
	2	8.2971	109.1056	4.0311	25	
	3	7.8929	101.6165	4.0311	25	
	4	7.3876	92.2551	4.0311	25	
	5	6.9021	81.015	5.9022	25	
	6	6.3968	71.6536	5.9022	25	
	7	5.8718	64.171	4.0311	25	
	8	5.3269	58.5672	0.289	25	
subj16		X	Y	Z	Label #	Group 1
	1	0.9647	98.0658	10.836	25	
	2	1.0441	94.3131	14.5824	25	
	3	0.917	88.6895	14.5824	25	
	4	0.7899	83.0659	14.5824	25	

	5	0.6627	77.4424	14.5824	25	
	6	0.5356	71.8188	14.5824	25	
	7	0.4085	66.1952	14.5824	25	
	8	0.1992	60.5735	12.7092	25	
subj17		X	Y	Z	Label #	Group 2
	1	12.1011	104.1904	5.2726	25	
	2	11.6941	100.4547	9.0147	25	
	3	11.3253	94.8405	10.8858	25	
	4	10.9565	89.2263	12.7569	25	
	5	10.7086	83.6067	12.7569	25	
	6	10.5816	77.9819	10.8858	25	
	7	10.3337	72.3623	10.8858	25	
	8	10.2066	66.7375	9.0147	25	
subj18		X	Y	Z	Label #	Group 2
	1	3.4609	140.5316	13.0519	25	
	2	3.9145	134.9194	16.7937	25	
	3	4.1888	127.4244	16.7937	25	
	4	4.4631	119.9295	16.7937	25	
	5	4.6134	112.4299	14.9228	25	
	6	4.8877	104.935	14.9228	25	
	7	5.1619	97.44	14.9228	25	
	8	5.2437	91.8142	13.0519	25	
subj19		X	Y	Z	Label #	Group 1
	1	2.5645	126.6846	0.0436	25	
	2	3.0135	121.0776	0.0436	25	
	3	3.3825	115.4641	1.9169	25	
	4	3.7514	109.8506	3.7901	25	
	5	4.1203	104.2372	5.6634	25	
	6	4.4892	98.6237	7.5367	25	
	7	4.9382	93.0167	7.5367	25	
	8	5.3873	87.4096	7.5367	25	
subj20		X	Y	Z	Label #	Group 2
	1	4.8697	111.1484	5.6784	25	
	2	5.1658	109.2503	13.1668	25	
	3	5.2362	105.4878	18.783	25	
	4	4.9597	97.99	22.5272	25	
	5	4.7	92.37	24.3993	25	
	6	4.2147	84.8858	24.3993	25	
	7	3.7294	77.4015	24.3993	25	
	8	3.2441	69.9172	24.3993	25	